Computer simulations of the diffusion of Na^+ and Cl^- ions across POPC lipid bilayer membranes

Rangeen Salih and C. C. Matthai

Citation: The Journal of Chemical Physics **146**, 105101 (2017); doi: 10.1063/1.4977703
View online: http://dx.doi.org/10.1063/1.4977703
View Table of Contents: http://aip.scitation.org/toc/jcp/146/10
Published by the American Institute of Physics

Computer simulations of the diffusion of Na^+ and Cl^- ions across POPC lipid bilayer membranes

Rangeen Salih[a] and C. C. Matthai
Department of Physics and Astronomy, Cardiff University, Cardiff, United Kingdom

(Received 14 December 2016; accepted 16 February 2017; published online 10 March 2017)

We have carried out molecular dynamics simulations using NAMD to study the diffusivity of Na and Cl ions across a POPC lipid bilayer membrane. We show that an imbalance of positively and negatively charged ions on either side of the membrane leads to the diffusion of ions and water molecules. We considered the cases of both weak and very strong charge imbalance across the membrane. The diffusion coefficients of the ions have been determined from the mean square displacements of the particles as a function of time. We find that for strong electrochemical gradients, both the Na and Cl ions diffuse rapidly through pores in the membrane with diffusion coefficients up to ten times larger than in water. Rather surprisingly, we found that although the Na ions are the first to begin the permeation process due to the lower potential barrier that they experience compared to the Cl ions, the latter complete the permeation across the barrier more quickly due to their faster diffusion rates. *Published by AIP Publishing.* [http://dx.doi.org/10.1063/1.4977703]

I. INTRODUCTION

Cellular membranes form a separation between the extracellular space and the intracellular fluid that is mostly impermeable. Lipid bilayers, which represent the core of all biological membranes, are self-assembled structures composed of amphiphilic lipids and water. Lipid bilayer membranes form a barrier to proteins, molecules, and many ions dissolved on either side of the membrane. In the previous studies, Matthai *et al.*[1,2] investigated the transport of biopolymers through channels made up of hemolysin pores embedded in a lipid bilayer membrane.

It is well known that ions like K^+, Cl^-, and Na^+ can and do permeate across the membrane. Although this selectivity in permeability is primarily based on size, other factors can influence the diffusion of ions across a membrane.

In any computer simulation study, the choice of interatomic force fields is of paramount importance. Over the years, there have been many attempts at deriving force fields that reproduce the structure and charge distributions of small molecules as calculated using *ab initio* quantum mechanical techniques. While none of these can hope to describe all the chemical processes accurately, the goal has been to construct force fields that are accurate enough but which can also be used for large scale simulations, both from the point of system sizes and simulation time.[3,4] In modelling the diffusion of atoms, ions, or molecules across the biological membranes it is therefore important to utilise force fields that reproduce amongst other things, the experimentally determined diffusion coefficients.

There have been numerous studies aimed at estimating the value of the self-diffusion coefficient, $D_S(H_2O)$, of water.[5–10] For example, Mills[10] using a tracer method and Holz *et al.*[9,10] using the pulsed magnetic field gradient (PFG) NMR both found an average value of $D_S(H_2O)$ to be about 2.2×10^{-5} cm^2/s. Computational studies, involving methods such as MD simulations, have also been carried out by numerous workers. Mark and Nilsson[11] used the TIP3P (transferable intermolecular potential 3P) force field model to carry out simulations on water at 298 K for 100 ps. Then, using different time trajectories they found the average value of the diffusion coefficient to be $D_S(H_2O) = 5.60 \pm 0.08 \times 10^{-5}$ cm^2/s. While this is larger than that found experimentally, it is in agreement with the results obtained from other computer simulation studies. Yeh and Hummer[12] also carried out computational investigations of the diffusion coefficient of water using the TIP3P model and found this to be 6.05×10^{-5} cm^2/s. Other force field models have also been used in this context. The SPC (extended simple point charge) model was used by Postma[13] who determined the value of $D_S(H_2O)$ to be 7.5×10^{-5} cm^2/s at 350 K.

The diffusion coefficient of water is greatly affected by the surrounding medium and in particular, when water is in the neighbourhood of a membrane or other large molecular systems. So, for example, López Cascales *et al.*[14] ran MD simulations on a charged biological membrane surrounded by water and measured the translational diffusion coefficient of water molecules in the bulk water region, but parallel to the membrane. They found $D_S(H_2O)$ to be greater than 8×10^{-5} cm^2/s. This is similar to the values obtained by Postma[13] using the SPC model.

It must be stressed that the values obtained for the self diffusion coefficient of water in computer simulations are very much dependent on the force field models used to describe the water-water interactions and it is now recognized that the TIP3P model generally gives larger values for $D_S(H_2O)$ than is found experimentally. However, in spite of these inconsistencies, there is a consensus that the TIP3P model gives a good description of the interaction of water with lipid

[a] Physics Department, School of Science, University of Sulaimani, Kurdistan region, Iraq.

membranes and so, in simulations involving water and biological membranes, it is often taken to be the force field model of choice.

There have also been many studies aimed at understanding the processes involving the diffusion of ions across the lipid bilayer membranes. Hardy *et al.*[15] carried out MD simulations of the diffusion of ions across a POPC lipid membrane immersed in a NaCl solution. Gurtovenko and Vattulainen[16] demonstrated the importance of asymmetry by performing MD simulations of asymmetric lipid membranes comprising zwitterionic (phosphatidylcholine (PC) or phosphatidylethanolamine (PE)) and anionic (phosphatidylserine (PS)) leaflets. They showed that the asymmetry in *trans*-membrane distribution of anionic lipids gave rise to a non-zero potential difference between the two sides of the membrane. This was a consequence of the difference in charges on the two leaflets.

It has also been suggested[17] that an imbalance of ions on either side of a lipid bilayer system could result in the creation of a water pore which in turn allowed for the passage of ions across the membrane until the charge equilibrium was established. In their MD simulations on a POPC lipid membrane surrounded by NaCl in water, Hardy *et al.*[15] introduced different ions on either side of the membrane and used semi-periodic boundary conditions. This resulted in an electric field of 0.7 V/nm being produced across the membrane which then allowed ions to diffuse through the pore and across the membrane.

In this paper, we report the results of investigations carried out to further our understanding of how the ion imbalance and the resulting electrochemical gradient across the bilayer affects the diffusion of water molecules, and of Na^+ and Cl^- ions. To this end, we have concentrated on using well tried and tested force fields which can be used reliably in simulating biological molecules in aqueous solution. We have determined the diffusion coefficients of the different particles inside and around the membrane both with and without the presence of an electrochemical gradient.

In Section II, we describe the systems constructed to model the diffusion of ions and water molecules across the POPC membranes. In Section III, we give a description of the computational methodology and the methods employed in the analysis of the data resulting from the simulations. In Sections IV, V, and VI, we report on the results of simulations on lipid bilayer membranes between aqueous solutions which are either the same or different on each side of the membrane. Finally, we conclude by comparing our results with those of other investigators and highlight the significant results of this study.

II. MODELLING THE DIFFUSION ACROSS THE LIPID BILAYER MEMBRANE

The lipid bilayer considered in this work was the POPC bilayer. Like all lipid bilayers, the POPC bilayer comprises 2 leaflets, each in turn made up of a number of phospholipid molecules. The phospholipid molecule has a hydrophilic head group and a hydrophobic tail group (Figure 1). Because of this, the heads of the molecule prefer to be in an aqueous environment, while the tails are more stable in a lipid environment. This then leads to the natural formation of bilayers in which the head groups point outwards into the water, while the tail groups point towards each other. When placed in water, these bilayers tend to form spherical shapes with water inside and outside the membrane (Figure 2).

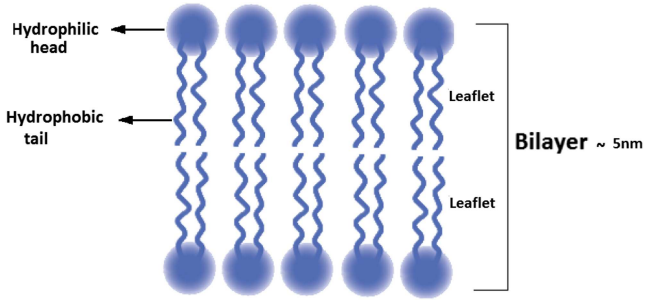

FIG. 1. Schematic diagram of a POPC lipid bilayer.

A. Systems

In order to simulate the flow of ions and water molecules across the membrane from the cytoplasm to the extracellular fluid, we modelled the system to be a lipid bilayer between two fluids, as shown in Figure 2.

In carrying out molecular dynamics simulations, it is efficacious to employ periodic boundary conditions, especially when performing the analysis of the electrostatic potential in the simulation cell. With such periodic boundary conditions, two different types of arrangements of the cell membrane between the cytoplasm and the extracellular fluid were configured. In the first arrangement, it is assumed that both fluids have the same constituents. In such a scenario, it is sufficient to model the system according to the simulation cell (labelled configuration I) as shown in (Figure 3(a)) with one bilayer surrounded by water molecules. When considering different fluids on the two sides of the membrane and still maintaining periodic boundary conditions, a two boundary arrangement (labelled configuration II) as shown in Figure 3(b) is necessary.

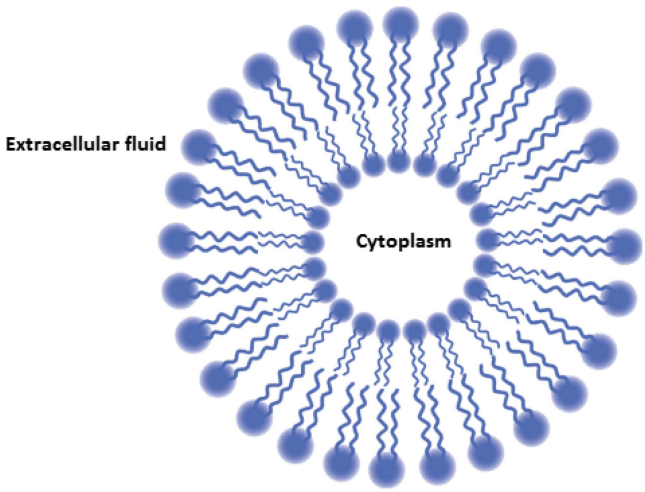

FIG. 2. Cell structure showing the cellular membrane enclosing the cytoplasm. The extracellular fluid is on the outside of the membrane.

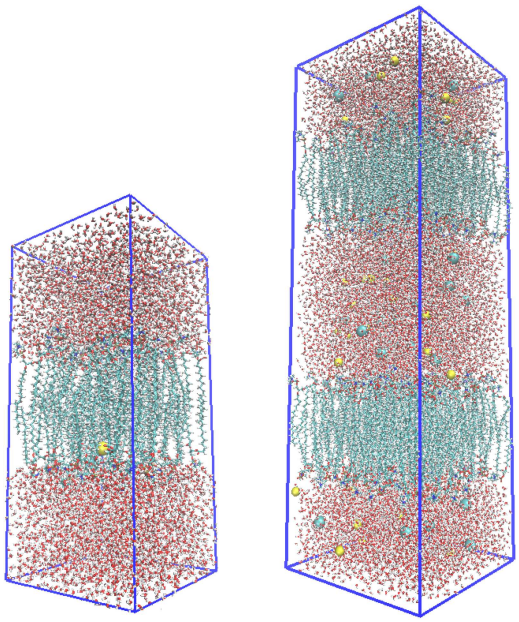

(a) Configuration I (b) Configuration II

FIG. 3. (a) Configuration I is used to model systems with the same fluid on either side of the membrane. (b) Configuration II is used to model systems with different fluids on either side of the membrane. The lipids forming the membrane, shown as chain molecules (gray), are surrounded by water molecules (red), Na ions (yellow), and Cl ions (cyan).

In each of these configurations, variations of the fluid constituents were considered. In all, five different systems were investigated. System A (see Table I) was configured with the intention of investigating the diffusion of single Na and Cl ions across a membrane surrounded by water. So for this system, the fluids on either side of the membrane were taken to be just water. System B was evolved from system A by adding NaCl to the water, making a weak saline solution, i.e., water with an equal number of Na and Cl ions in each fluid. System C was configured to examine the effect of having unequal numbers of sodium and chlorine ions, thus making it a charged fluid. The final two systems (system D and system E) were constructed to order to investigate the scenarios in which there are different fluids on either side of the membrane. The details of these systems are given in Table I.

III. COMPUTATIONAL METHODOLOGY AND ANALYSIS

A. Molecular dynamics simulations

In order to determine the diffusion coefficients of the ions and the water molecules across the lipid bilayer, systems comprising either a lipid single bilayer membrane or a double bilayer, as shown in Fig 3, surrounded by water molecules and including a few of the relevant ions of interest were set up. All the atoms and molecules were confined to a three-dimensional periodically repeating molecular dynamics simulation box as shown in Figure 3. The simulation box was taken to have tetragonal symmetry with dimensions as given in Table I.

The lipid bilayers and the surrounding water molecules were built by using the visual molecular dynamics (VMD) package.[18] All the molecular dynamics simulations were carried out using the NAMD 2.10 package.[19]

The systems were kept in an isothermal-isobaric (NPT) ensemble at a pressure of 1 bar using a modified Nose-Hoover method.[20] The van der Waals and Coulomb interactions were cut-off at 12 Å and the particle mesh Ewald (PME) method was used to carry out the calculations of the long-range Coulomb interactions[21] with a grid point density of 1.2 $Å^3$. The interatomic forces between the atoms in the lipids and the water molecules were taken to be that described by the CHARMM36[22] force fields and the water TIP3P force field model.[11] For the interactions of the sodium and chlorine ions with water and with the lipid atoms, the Lennard-Jones parameters used in the CHARMM36 force fields are given in Table II.

In each simulation study, the systems considered were first allowed to reach their minimum energy configuration. This was done by carrying out a MD run over at least 5000 time steps, each of 2 fs. Subsequently, using Langevin dynamics, the systems were allowed to reach a dynamical equilibrium configuration at 300 K. A Langevin damping coefficient of 1 ps^{-1} was used to control the temperature. After dynamical equilibrium was achieved, the simulation was allowed to run for 50 to 65 ns and the resulting time averaged configurations were subject to analysis.

TABLE II. Lennard Jones parameters for the ions in CHARMM36 and used in this study.

Ions	ϵ (kcal/mol)	$R_{min}/2$ (Å)
Na^+	0.0469	1.36375
Cl^-	0.150	2.27

B. Area per lipid and bilayer thickness

The area per lipid (APL) of a bilayer provides much important information about a bilayer or a membrane. As the APL effectively measures the equilibrium spacing between the head

TABLE I. The systems investigated in the molecular dynamics simulations are identified by a system label. For each system, the configuration type (as shown in Figure 3), the simulation box size, the number of molecules, and the fluid constituents are tabulated.

System label	Configuration type	Size $Å^3$	Number of molecules	Fluid 1	Fluid 2
A	I	$50 \times 50 \times 110$	59 lipids + 6388 H_2O	H_2O + Na^+ (or Cl^-) ion	
B	I	$72 \times 72 \times 120$	136 lipids + 10 836 H_2O	H_2O + 20 Na^+ + 20 Cl^-	
C	I	$72 \times 72 \times 120$	136 lipids + 10 836 H_2O	H_2O + 15 Na^+ + 25 Cl^-	
D	II	$72 \times 72 \times 200$	272 lipids + 18 211 H_2O	H_2O + 19 Na^+ + 21 Cl^-	H_2O + 18 Na^+ + 17 Cl^-
E	II	$72 \times 72 \times 200$	272 lipids + 18 211 H_2O	H_2O + 50 Na^+	H_2O + 50 Cl^-

groups (and also between the tail group molecules), it is sensitive to any changes in the interaction between the head group molecules. The interaction between head group molecules is in turn dependent of their interaction with the ions and molecules in the aqueous solution. Thus, an accurate determination of the APL is desirable as this would imply that the 2-D density in the bilayer plane is correctly described. This is essential in having confidence that the simulation correctly predicts other structural properties, such as the lipid tail order parameters, the bilayer thickness (BLT), the electron density profiles, as well as the overall phase behaviour of the membrane. The bilayer thickness is another important quantity that needs to be monitored to ensure the robustness of the simulations.

The APL and the BLT have been measured both experimentally and determined by computational methods for different types of lipid bilayer membranes. X-ray measurements of the thickness of the POPC membrane have been reported to be approximately 37.0 Å. The experimental values of the area per lipid have been found to vary quite considerably. For POPC, values between 54 Å and 68 Å^2 have been reported.[23] The computationally determined values are of course dependent on the choice of the force fields. Klauda *et al.*[24] have reported the area per lipid of the POPC using CHARMM 36 to be 64.7 Å^2. In all our simulations, the BLT values for the POPC bilayers were found to be approximately 38.5 Å. This is in general agreement with the experimental values.

It is important to note that the APL and BLT are also dependent on the fluids surrounding the membrane. Thus, increasing the NaCl concentration in the fluids results in an increase in the bilayer thickness. Correspondingly, the area per lipid decreases. These variations may be attributed to polarization effects and to atomic displacements in the bilayer.

In the event of pore formation in the membrane, the APL has been reported to show a sharp increase in its value and there is a corresponding decrease in the lipid thickness in the region of the pore. This comes about as a consequence of the redistribution of the headgroup molecules towards the pore interior. By comparing the computational values with experimental results, it is therefore possible to confirm the reliability of the results of simulations.

C. Calculation of the diffusion coefficients

The diffusion coefficient, D, is a measure of the speed of the translational motion of particles through a particular medium and is one of the many dynamic properties of a molecule in solution. It depends not only on the size and shape of the molecule and its interaction with the surrounding medium but also on the temperature of the system. The diffusion coefficient can be determined from molecular dynamics simulations by analysing the molecular (or atomic) trajectories as a function of time. It is assumed that these particles undergo Brownian motion which is a stochastic process reflecting the motion of particles due to thermal collisions with the solvent molecules.[25] The diffusion coefficient, D, is related to the time averaged mean square displacement of a particle moving in d dimensions through the equation,

$$D = \lim_{t\to\infty} \frac{1}{2dt} \left\langle (\mathbf{r}(0) - \mathbf{r}(t))^2 \right\rangle, \qquad (1)$$

TABLE III. Diffusion coefficients, D ($\times 10^{-5}$ cm^2/s), of Na^+ and Cl^- ions at different positions in the simulation box for system A. Also shown is the diffusion coefficient for a water molecule.

Position in the simulation box	$D(Na^+)$	$D(Cl^-)$	$D(H_2O)$
In the lipid hydrophobic region	0.1	1.4	2.9
On top of the lipid hydrophilic region	0.3	1.8	4.9
In the bulk water region	1.6	2.2	5.3

where $\mathbf{r}(t)$ is the position of the molecule at time t. The term in the angular brackets in the above equation is often referred to as the mean square displacement (MSD). Although for very short times, the MSD fluctuates with time in a non-linear fashion, over longer times there is a linear relationship from which D can be determined. Hence, D is given by the slope of a plot of the MSD against time divided by twice the system dimension (e.g., 2 for linear, 4 for lateral, and 6 for bulk diffusion). In our calculations of the MSD of the ions and water molecules, we have used a 1 ns time-window with positions tabulated every 0.004 ns.

D. The electrostatic potential across the membrane

An important quantity that determines the viability of molecular diffusion across a membrane is the electrostatic

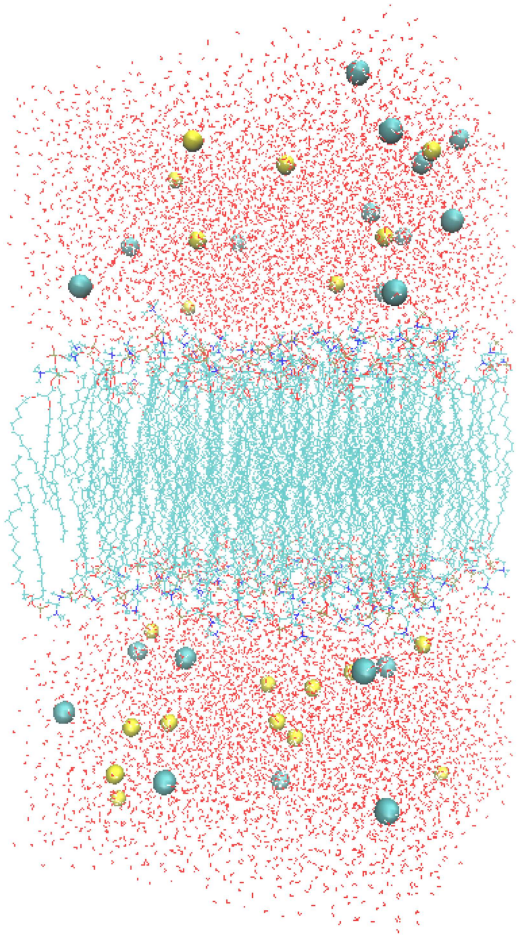

FIG. 4. The simulation cell with a single POPC lipid bilayer surrounded by water containing equal numbers of Na^+ (yellow) and Cl^- (cyan) ions.

potential, $\phi(z)$ across the lipid bilayer, where z is the coordinate perpendicular to the membrane surface. The electrostatic potential is obtained by numerically solving Poisson's equation

$$\nabla^2\phi(\mathbf{r}) = -\frac{1}{\varepsilon_0}\sum_i \rho_i(\mathbf{r}), \tag{2}$$

where ε_0 is permittivity and the charge density around every ion in the system is approximated by a spherical Gaussian charge distribution as

$$\rho_i(\mathbf{r}) = q_i\left(\frac{\beta}{\sqrt{\pi}}\right)^3 e^{-\beta^2|\mathbf{r}-\mathbf{r}_i|^2}. \tag{3}$$

The charges, q_i, are obtained directly from NAMD simulations and β depends on the size of the ions.

In our simulation studies, VMD was used to calculate the mean electrostatic potential from the grid points. This was done by using the smooth particle mesh Ewald method (SPME)[26] to generate a smooth electrostatic potential grid controlled by the Ewald factor. From the above equations, the mean electrostatic potential is found by averaging the instantaneous electrostatic potential $\phi(r)$ over the entire trajectory of the MD simulations. The potential across the membrane is then obtained by taking an average over the membrane surface (x, y) plane.

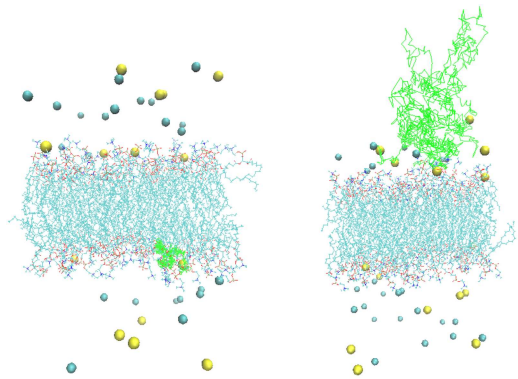

(a) Na ion (b) Cl ion

FIG. 5. Typical trajectories (in green) over 10 ns of (a) Na^+ (yellow) and (b) Cl^- (cyan) ions in the simulation system B.

IV. SIMULATIONS OF SINGLE Na^+ AND Cl^- ION INTERACTIONS WITH A MEMBRANE SURROUNDED BY WATER

In order to investigate the interaction of single ions with the membrane and the possible diffusion of Na^+ and Cl^- ions across a lipid bilayer membrane, a POPC membrane

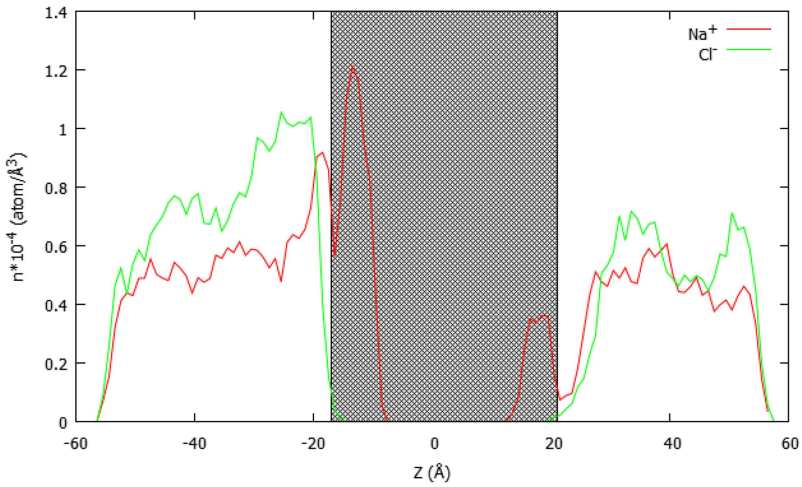

(a) System B

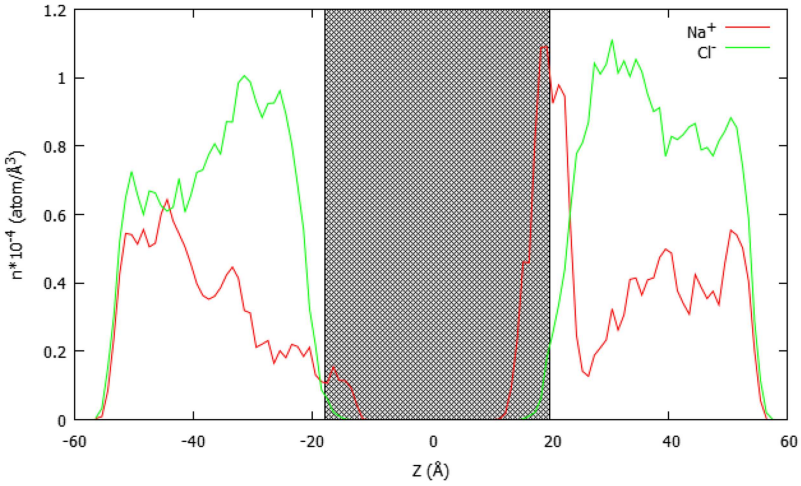

(b) System C

FIG. 6. Time averaged density distribution (vertical axis) of Na (red lines) and Cl (green lines) ions in the simulation systems B (a) and C (b) as a function of position across the simulation cells. The bilayer regions are indicated by the shaded areas.

comprising 59 lipid molecules, with 29 in the upper leaflet and 30 in the lower leaflet, was constructed and placed in the middle of the simulation box. The number of lipids in each leaflet was determined by the dimensions of the simulation box. Above and below the membrane, 19 161 water molecules were randomly sited, as shown in Figure 3(a). Then, a single Na^+ (or Cl^-) ion was positioned at different sites inside and just outside the membrane layer (Figure 3(a)). For each of these ion starting positions, the simulation was allowed to run at 300 K and the trajectory of the ion monitored.

When a Na^+ ion was placed in the hydrophobic region (just below the head groups) of the lipid bilayer POPC membrane, it took just under 4 ns before it moved out of the membrane and a further 4 ns before it moved into the bulk water region of the assembly. The diffusion coefficient of the ion in the three regions, inside the membrane, at the membrane surface, and in the bulk water, was determined from the MSD plots and the results are shown in Table III. The low diffusion coefficient of the ion whilst inside the membrane is indicative of the relatively strong local binding of the ion with the surrounding atoms of the lipid molecules. As the simulation proceeds, entropy effects soon overcome this interaction energy and the ion is released and diffuses out of the membrane surface into the surrounding water.

When the ion is in the surface region of the bilayer membrane, it diffuses much more rapidly which is consistent with a smaller interaction energy between the ion and the bilayer surface. When the ion finally moves into the bulk region of the water, the diffusion coefficient of the Na^+ ion is similar to its value in water with no membrane present. This value of the diffusion coefficient is in reasonably good agreement with the experimental finding of 1.33×10^{-5} cm^2/s.[27]

As mentioned above, the stability of the equilibrium values of the APL and BLT gives a measure of the confidence in the simulations. In the simulations with a single Na^+ added to the system, the APL was found to be 79 ± 3 $Å^2$ which is larger than the experimentally observed value for this system. The BLT was found to be 32 Å which in turn is slightly smaller than the experimental value for the POPC bilayer.

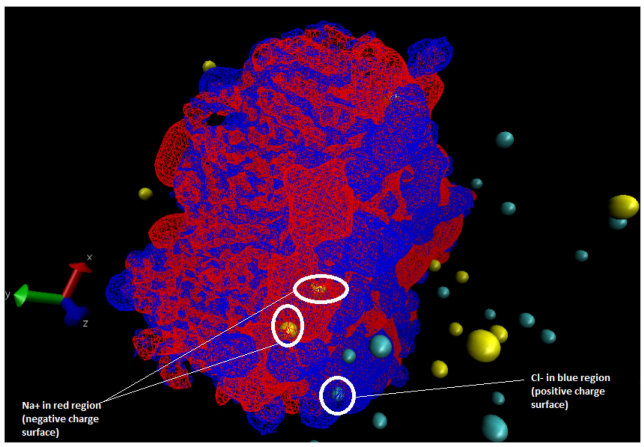

FIG. 7. The net charge distribution on the lipid bilayer. The red areas are regions of negative net charge, while blue is of net positive charge. Also shown are the positions of the Na and Cl ions.

When a Cl^- ion was similarly placed at specific positions in the hydrophobic region (just below the head groups) in the lipid bilayer POPC membrane, the ion immediately moves out of the lipid, carrying out a random walk around the lipid membrane surface before moving into the bulk water region. The diffusion coefficient, both at the surface of the lipid bilayer and in the bulk water region, is close to the experimentally observed value of 2.03×10^{-5} cm^2/s.[28]

From these simulations, it is clear that while there is a tendency for a Na ion to be partially bound inside but near to the bilayer surface, it is easily displaced out of its binding site. In contrast, the Cl ion is not bound to any of the sites at or below the bilayer surface.

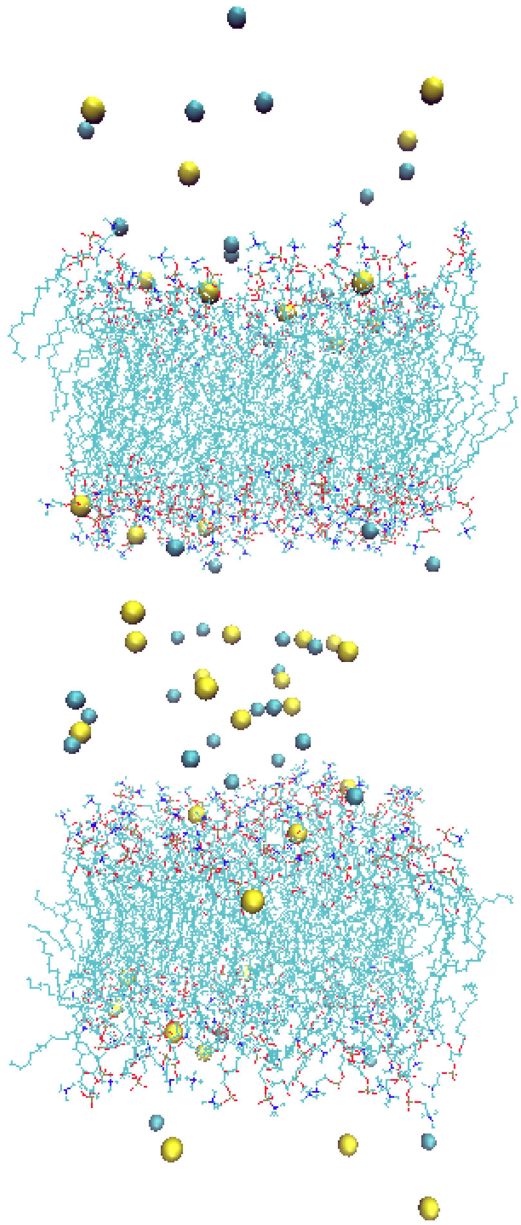

FIG. 8. Figure showing the ion distribution in system D after 50 ns together with the two POPC lipid bilayers. The water molecules are not shown in order to highlight the positions of the Na (yellow) and Cl (blue) ions. The lipid bilayer is shown as chains. Note the presence of a Na ion inside the lipid bilayer.

V. SIMULATIONS OF SINGLE Na^+ AND Cl^- ION INTERACTIONS WITH A MEMBRANE IMMERSED IN AN IONIC SOLUTION

In order to investigate the effect of changing the fluid constitution surrounding the lipid bilayer membrane, the systems were modified by adding Na^+ and Cl^- ions to the water surrounds. Two sets of such simulations were carried out. In the first (system B), equal numbers (20) of Na^+ and Cl^- ions were introduced, while in the second set (system C), an imbalance in the ions (with 15 Na^+ and 25 Cl^- ions) was created to see how the non-neutrality of the fluid affected the ion-membrane interactions.

The simulation details for these systems are given in Table I. The sizes of these systems (POPC lipids in a box of TIP3P water) were larger than that in system A. This was to allow for the random distribution of the 40 ions in the surrounding water. The number of lipids in each of the upper and lower leaflets was increased to 136. This meant that there were a total of 18 224 atoms in the membrane and 32 508 atoms in the water in addition to the 40 Na^+ and Cl^- ions randomly distributed in the water, and initial molecular configuration for system B is shown in Figure 4. Once again, the simulations were run for 50 ns over which the APL, the BLT, and the diffusion coefficients of the specific ions were determined.

A. APL and BLT

The BLT after equilibration for both systems was found to be just under 38 Å. This is in good agreement with the experimental measurement of 37.0 Å found for POPC using X-ray scattering.[23] Kuerka *et al.*[23] also found that the APL varied between 54 and 68.3 $Å^2$. The APL has also been determined computationally by many other researchers. For example, MD simulations on POPC using CHARMM force fields was found to give an APL of 64.7 $Å^2$.[24] Comer *et al.*[29] investigated how the APL was affected by using different van der Waals cutoffs. They found that for cutoffs between 1 and 1.2 nm, the APL was about 65 $Å^2$. It has also been observed that the APL depends on the number of Na and Cl ions in the simulation cell.[30] Interestingly, it was found that an increase in the NaCl concentration led to a decrease in the APL. In our simulations with a total of 40 Na and Cl ions, the APL was found to be 67.3 ± 1.5 $Å^2$. These APL and BLT values are in good agreement with experimental measurements on real systems indicating that both systems were of optimal size and had reached a full thermal equilibrium configuration after 50 ns.

B. Ion diffusion coefficients and their spatial distribution

While all the ion trajectories show the particles undergoing Brownian motion in the bulk water region, a substantial fraction of Na ions get close to the lipid surface and tend to remain there for a period of up to 10 ns. By contrast, the Cl ions tend not to adhere to the membrane surface and in general do not spend any substantial time close to the surface. These observations are similar to that reported by Miettinen *et al.*[31] and Sachs and Woolf.[32] Examples of typical trajectories for both Na and Cl ions in the simulation system B are shown in Figure 5.

The diffusion coefficients of the Na and Cl ions for both systems were computed from the MSD of the ion trajectories. While the ions in the bulk water region had similar diffusion coefficients to that given in Table III, the Na ions at the surface region or inside the membrane bilayer have much reduced values. In determining this, all the Na ions near or below the surface were sampled at different time intervals. All of these samplings gave results of $D(Na^+) \approx 0.1 \times 10^{-5}$ cm^2/s, for ions at or below the bilayer surface. Thus, it may be concluded that the NaCl aqueous solution has the effect of allowing the Na ions to penetrate the membrane more deeply and to remain inside for longer periods.

We have also monitored the ion density distribution across the simulation cell over the simulation period and the results for both system B and system C are shown in Figure 6. The shaded region in the figures depict the membrane bilayer with its edges at approximately −18 Å and 20 Å. This corresponds to the bilayer thickness of approximately 37 Å. It is interesting to note that for both systems, there are always some Na ions just at or below the headgroup of the membrane. However, no Cl ions are found below the membrane surface for any significant time period. On integrating out the area under the curves, we find that for system B on average, 4–5 Na ions out of the total of 20 Na ions are to be found near or below the membrane surface. Similarly for system C, about 3 Na ions

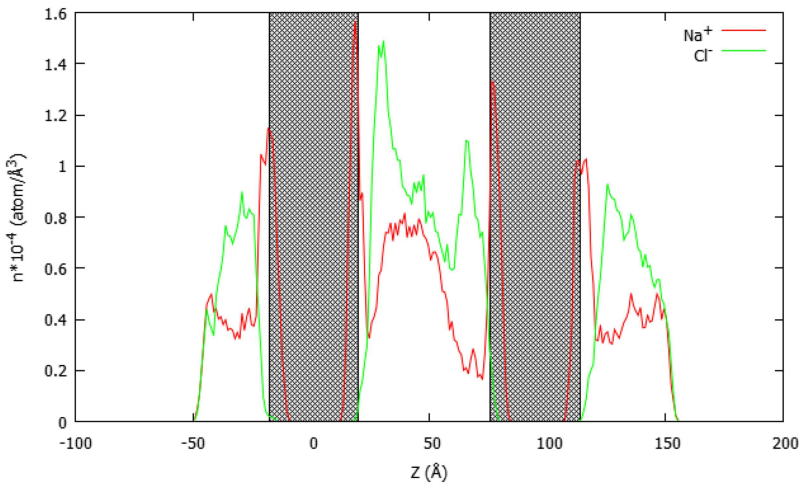

FIG. 9. The time averaged number density of both ions as a function of the z-axis for system D. The bilayer regions are indicated by the shaded areas.

out of the 15 spend considerable time at or below the bilayer surface. So, for both systems, more than 20% of the Na ions are to be found at or below the bilayer surface. In contrast, for system B, there are no Cl ions at or below the membrane surface. For system C, which had a higher concentration of Cl ions, on average just one of these ions is found near the surface.

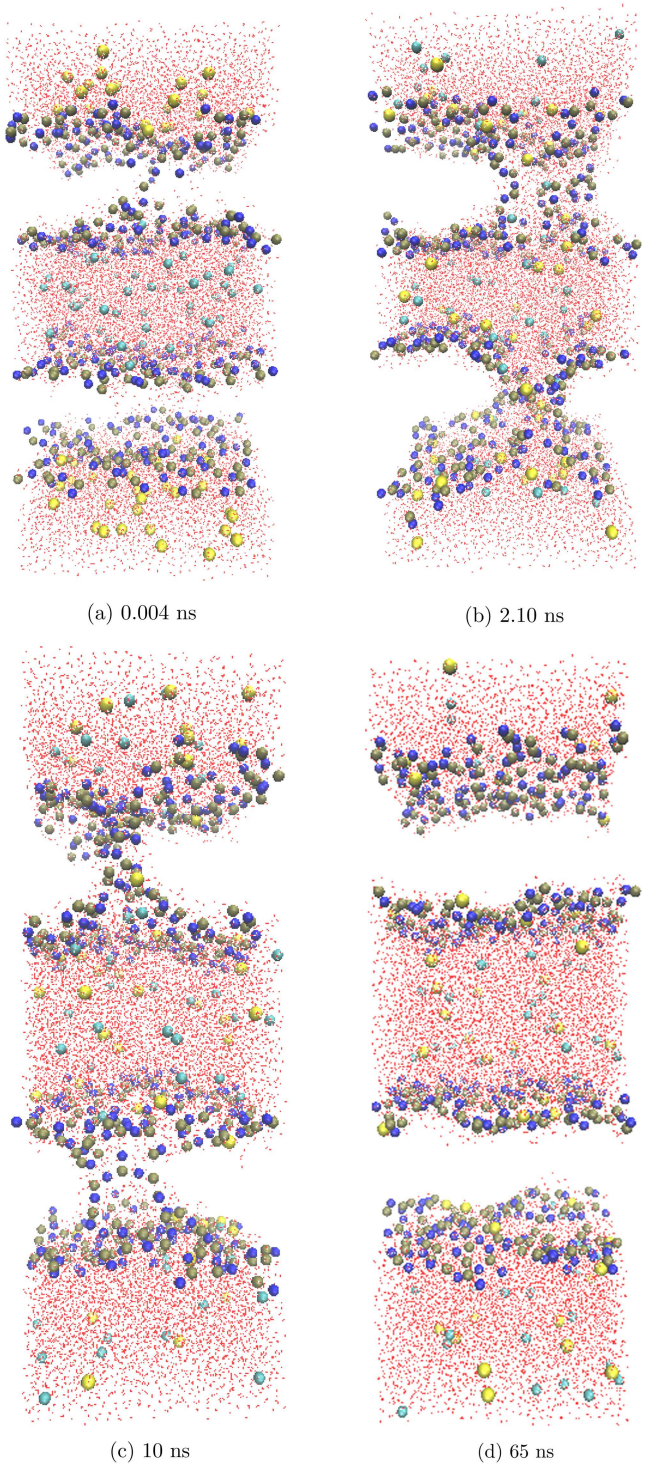

(a) 0.004 ns (b) 2.10 ns

(c) 10 ns (d) 65 ns

FIG. 10. Figure showing the water molecules and ion distribution in system E at different times of the diffusion process. Here, the Na ions are coloured yellow and the Cl ions cyan. The atoms comprising the two POPC lipid bilayers are not shown in order to highlight the opening up of the pore.

In order to explain this observation, we calculated the net charge distribution on the lipid bilayer membrane surface surrounded by water, but without the presence of any ions. The net surface charge distribution is shown in Figure 7. It is clear that the large areas of negative charge act as attractors for the Na ion while repelling the Cl ion. These have been identified as the carbonyl groups in the membrane. The binding of the Na ions to these carbonyl groups manifests itself in the very small diffusion coefficients for the Na ion.

Based on the diffusion coefficients, the ion trajectories, and binding sites, it appears that the introduction of ions into the aqueous surrounds has the effect of allowing the Na ions to penetrate more deeply and remain inside the membrane for longer periods of time. It is of interest, therefore, to examine how the presence of ions in the aqueous surrounds affects the charge density distribution of the bilayer.

VI. DIFFUSION OF IONS ACROSS A POPC LIPID BILAYER MEMBRANE WITH DIFFERENT FLUIDS ON EITHER SIDE

Having established that there is little or no likelihood of ion diffusion across a membrane when the fluids on either side of the membrane have the same constituents, following the work of Hardy *et al.*[15] and Gurtovenko and Vattulainen,[17] we focused on investigating the effects of introducing an ion imbalance across the bilayer. This is, of course, akin to introducing an electrochemical gradient across the membrane.

In order to model a membrane with different fluids on either side while keeping periodic boundary conditions, it is necessary to introduce two bilayers in the simulation cell. Then, the region between the two bilayers could represent the cytoplasm inside the cell (Figure 2), while the fluid outside the two bilayers would correspond to the extracellular fluid. Each of the two POPC lipids bilayers, comprising 68 upper and 68 lower leaflets, making a total of 272 lipid molecules, was constructed and placed in the simulation cell (see Figure 3(b)). The bilayers were separated by 60 Å of water molecules and corresponds to fluid 1 in Table I. The thickness of the Fluid 2 region was taken to be the same as that of the Fluid 1 region. Na^+ and Cl^- ions were then introduced into both of the fluid regions.

It has been reported[15,17] that the strength of the electrochemical gradient is a crucial parameter in allowing for ion diffusion across a bilayer. We have considered two extremes of this scenario. In the first, the charge imbalance was made to be small, with 19 Na^+ and 21 Cl^- ions in the inner region while having 18 Na^+ and 17 Cl^- in the outer fluid region. The net charge imbalance is therefore just a single electron charge. In the other scenario, in one fluid only Na^+ ions were introduced while in the other only Cl^- ions were positioned. We have labelled these two scenarios as system D and system E with the details of the computational cell given in Table I.

MD simulations were then carried out on both systems with a view to investigating the circumstances under which ion diffusion takes place, particularly to determine the electrochemical field gradient required for ion diffusion leading to the neutralising of the inner and outer fluids.

A. Results of simulations of system D

After the initial energy minimization of the system, the simulations were run for a total of 50 ns. After 10 ns, a substantial fraction of the sodium ions was found to move close to the membrane surfaces from both sides of the membrane. However, no ion appears to overcome the barrier to diffuse through the membrane. The MSD data were used to determine the ion diffusion coefficients at different times during the simulation. Whilst in the hydrophilic headgroup region of the lipid bilayers, the diffusion coefficient of the Na ion, as determined from its trajectories, indicates that it is roughly the same as it was in the simulations of system B, viz., around 0.1×10^{-5} cm^2/s. This again points to the field gradient not being strong enough to allow for easy diffusion across the bilayer.

However, it is clear that the effect of the potential gradient on the sodium ions is stronger than that on the Cl ions, and after 40 ns of the simulation, there is the first indication of a Na^+ ion beginning to move across the bilayer. In Figure 8, which shows the instantaneous position of the ions after 50 ns of the simulation, the presence of a single sodium ion deep inside the membrane is clear. By contrast, none of the chlorine ions are able to overcome the barrier at the surface of the membrane. It is also clear that the Na and Cl ions are distributed randomly over both fluid regions.

In Figure 9, we show the time averaged number density for both sets of ions across whole of the simulation box. As was found for the simulations with just one type of fluid, we note that there is a high incidence of sodium ions near to the lipid surfaces while the chlorine ions prefer to move in the water region and away from the membrane. Again, integrating out the areas under the curves, we found that roughly 20% of the Na ions are at or below the surface of the double bilayers. So, even though an electrochemical gradient has been established, it appears not to be strong enough for the ions to overcome the barrier for diffusion across the bilayers.

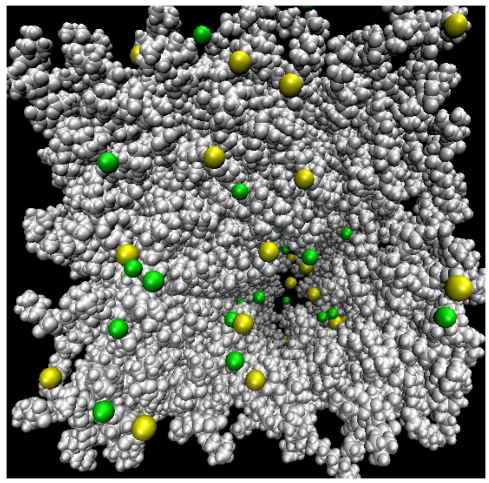

FIG. 11. Top view of the membrane showing the pore that allows for the passage of ions and water molecules through the membrane.

B. Results of simulations of system E

It has been suggested that[33] the permeation barrier for both Na and Cl ions in simulations of this size is too large for the observation of ion diffusion events. It is also clear that the

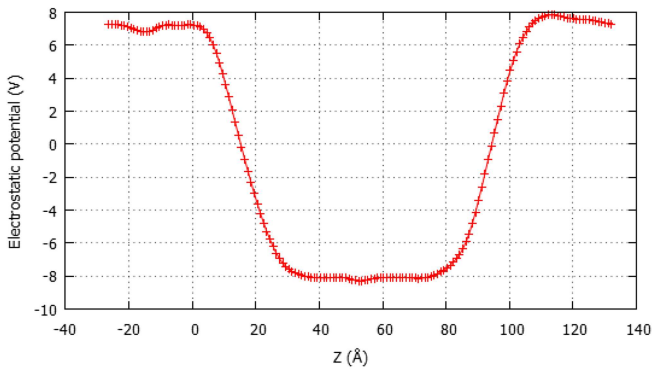

(a) t = 0.004 ns

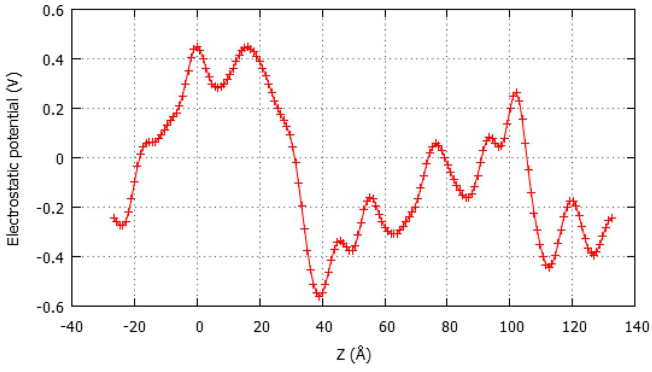

(b) t = 2.10 ns

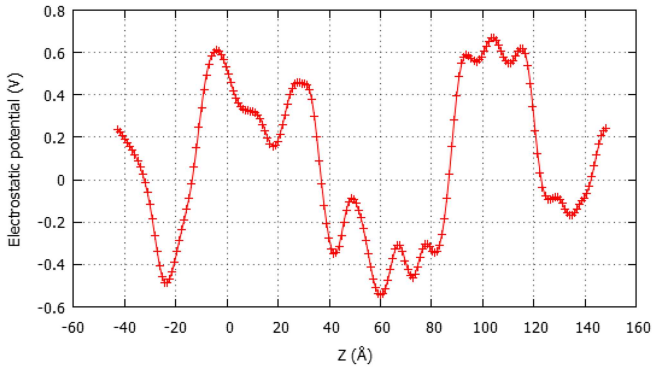

(c) t = 10 ns

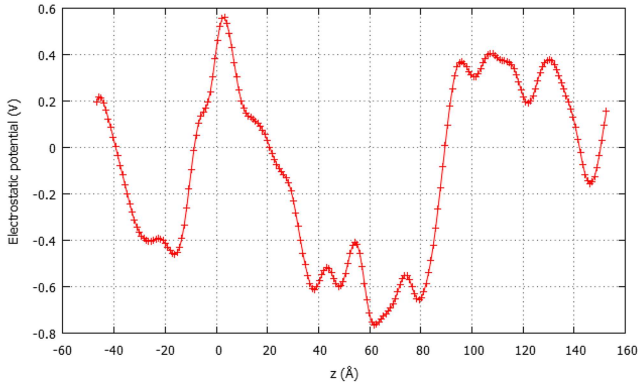

(d) t = 65 ns

FIG. 12. Electrostatic potential map across the two bilayers (horizontal axis) at different times, *t*, for system E. The vertical axis is along one of the cell edges parallel to the bilayer membrane surface.

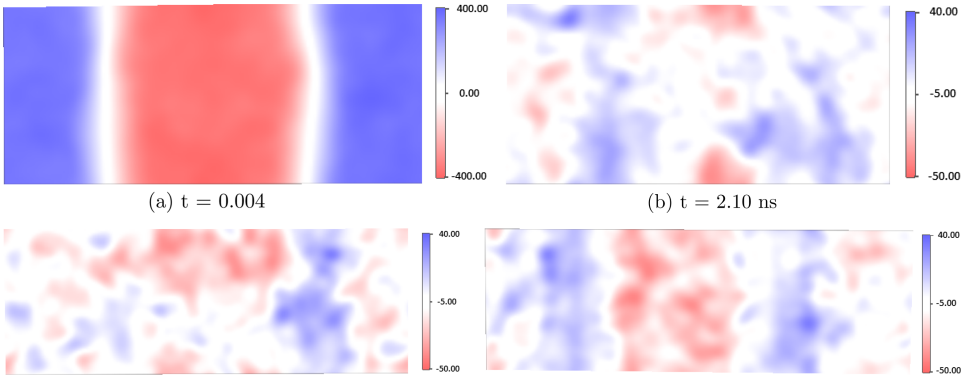

(a) t = 0.004 (b) t = 2.10 ns

(c) t = 10 ns (d) t = 65 ns

FIG. 13. Electrostatic potential map (x-z plot) across the two lipid bilayers at different times, t, for system E.

lack of diffusion across the bilayer in system D over time scales that are computationally feasible is a consequence of the weak electrochemical gradient. So, in order to speed up the diffusion process, it was decided to construct a system (system E) with a much stronger electrochemical potential gradient. This was generated by placing 50 Na^+ ions in the inner fluid region and 50 Cl^- ions in the outer fluid region.

The molecular dynamics simulations were then carried out as described above for the other systems. In a very short time, less than 0.004 ns of starting the simulation, water molecules break through the membrane and create what is referred to as a water pore. The evolution of the pore and the transference of ions from one fluid the other, across the membrane, can be seen in the snapshots at particular times of the simulation (see Figures 10 and 11). At the end of the simulation run of 65 ns, final distribution of the ions, shown in Figure 10(d), suggests that near charge equilibrium has been re-established.

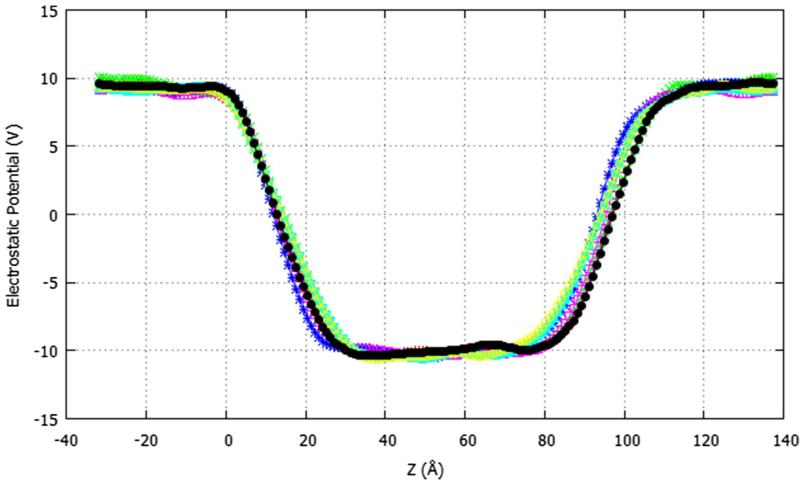

(a) t = 0.002 ns

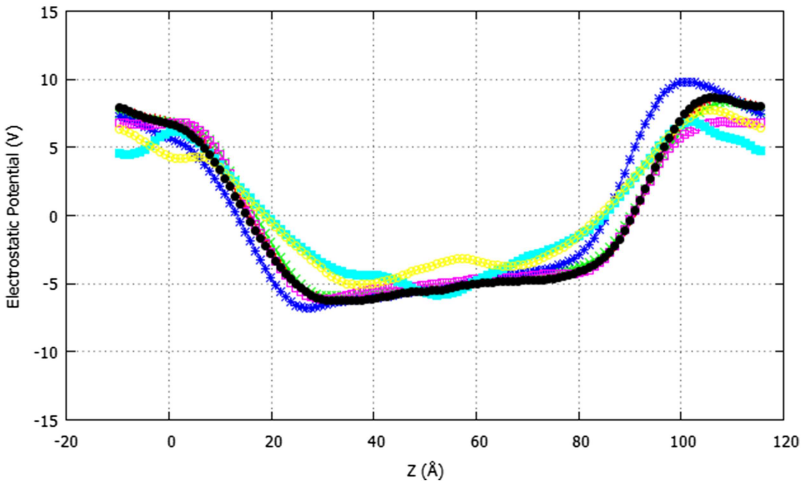

(b) t = 0.02 ns

FIG. 14. Electrostatic potential profiles at different times, t, as a function of distance across the two bilayers for system E. The bilayer edges are at approximately −7 Å, 30 Å, 88 Å, and 126 Å. The different colours denote the different coordinates (x,y) on the bilayer surface.

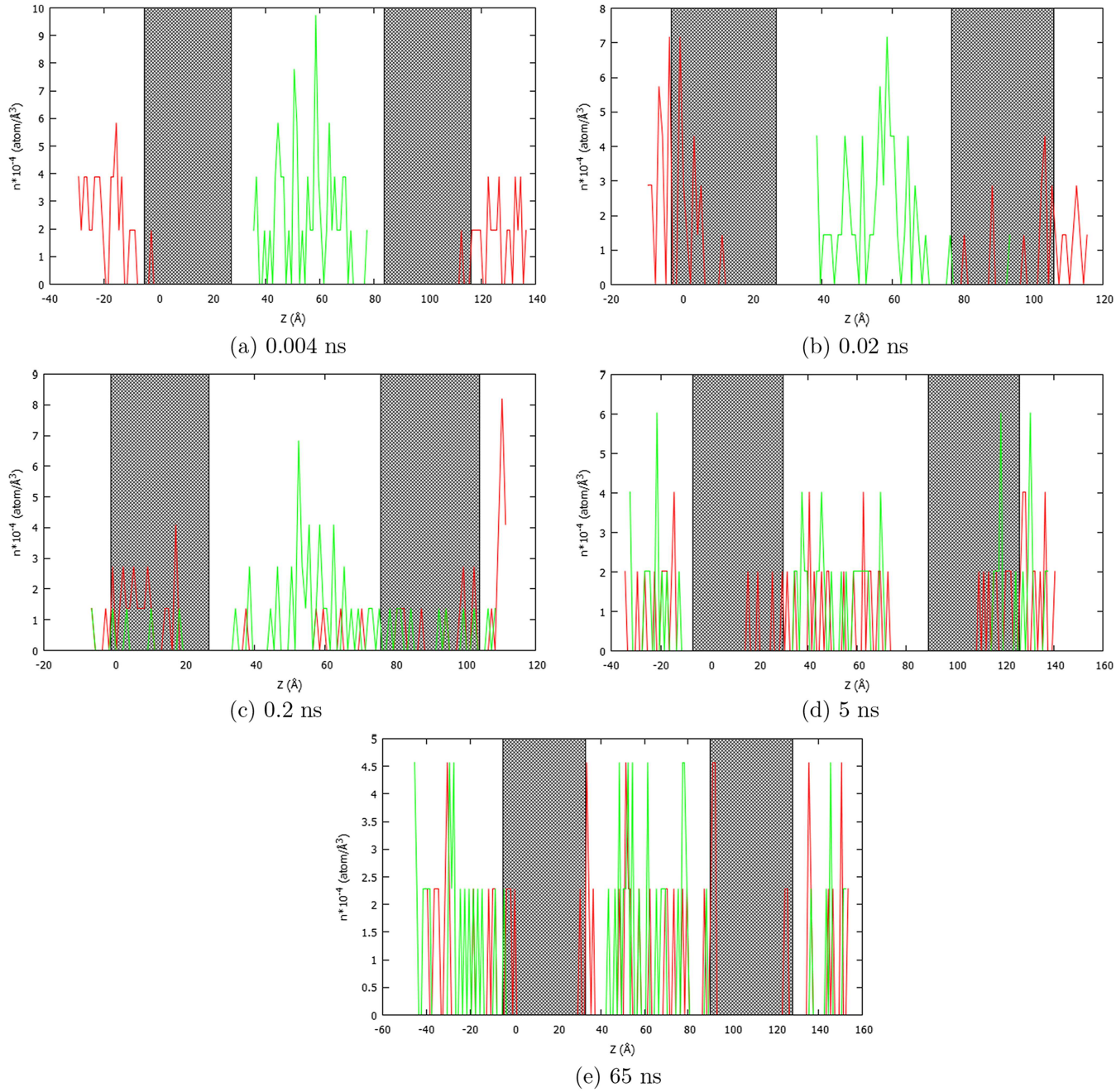

FIG. 15. The number of Na^+ (red) and Cl^- (green) ions across the simulations cell at specific times. The shaded areas represent the extent of the bilayers.

The electrostatic potential energy over a three dimensional grid of the simulation box was also calculated. In Figure 12 is shown the potential profile across the two bilayers averaged over the lateral positions at the time steps corresponding to the simulation times in Figure 10. It is interesting to note from these plots that there is a dramatic reduction in the strong electric field gradient within the first 2.1 ns after which the changes are relatively minimal. However, after 65 ns, there is still a small field gradient between the two bilayers.

To analyse this further, we have also plotted the electrostatic potential map in the cross section of cell (Figure 13) at these different time steps. These confirm the changes in the electrostatic potential spread right across the membrane and are not just confined to the pore region.

Interestingly, the potential profiles across the membrane at different (x, y) positions look remarkably similar (Figure 14). This is rather surprising as the electrostatic map in Figure 13 suggests that there are quite important differences at different lateral positions. At the start of the simulation, they are

TABLE IV. Diffusion coefficients, D ($\times 10^{-5}$ cm^2/s), of H_2O molecules, Na^+ and Cl^- ions at different times during their passage through the pore.

	$D(Na^+)$	$D(Cl^-)$	$D(H_2O)$
0.022 ns (in pore)	42.2	76.2	22.9
10 ns (in pore)	1.3	1.9	2.5
10 ns (in bulk water region)	1.7	2.6	5.0

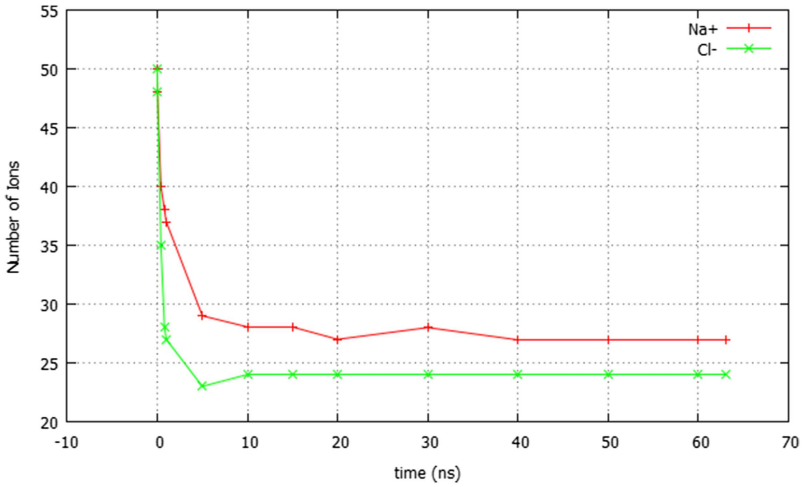

FIG. 16. Showing the reduction in the ion numbers for both Na and Cl in each of the fluid regions I and II, respectively, as a function of time. The difference between the two at the end of the simulation points to the cessation of ion diffusion when the electrochemical potential is small.

virtually identical. However, once a pore is formed, deviations in the profile tend to reflect the atomic displacements of the lipid molecules and the consequential charge density changes.

In order to examine the flow of ions across the membrane in a more detailed manner, we have plotted the number density of both Na and Cl ions across the simulation cell at different times (Figure 15). It is clear from these that the Na ions are the first to penetrate into the membrane. This happens to a substantial degree within the first 0.02 ns. However, it does not take much longer for the Cl ions to also move through the membrane so that within 5 ns of the start of the simulation, most of the ions (Cl and Na) have already moved onto the other side of the membrane to establish near charge neutrality.

Gurtovenko and Vattulainen[17] found the rather surprising result that both positive and negative ions leaked across the membrane in approximately the same ratio despite the fact that Na ions have a lower potential barrier for permeation through the pore. Our results suggest that this lower potential barrier is responsible for the Na ions being the first to penetrate, but following this, the Cl ions move through the membrane much more rapidly. We have calculated the diffusion coefficients from the MSD data obtained from the ion trajectories and these are given in Table IV. The values of D for both ions in the bulk region are similar to that tabulated in Table I. However, as the ions move through the pore, these values are greatly enhanced to more than 10 times as fast as in water. It is clear from this that the ions have very little interaction with any atoms or ions whilst in the pore. Interestingly, the Cl ions have a much higher diffusion coefficient than the Na ions, in spite of their grater mass.

A confirmation of this result can be seen in the plot of number of ions in each of the fluid regions (Figure 16). While from the results in Figure 15, it is clear that although the Na ions are the first to permeate the membrane, once the Cl ions start to move, they diffuse at a faster rate and to such an extent that they reach equilibrium more quickly than do the Na ions.

From the results of these simulations, we have found that if a large enough electrochemical potential gradient is established across the lipid bilayer membrane, both Na and Cl ions are able to permeate across the membrane. The relatively lower potential barrier experienced by the Na ions means that these are the first to start the diffusion process. However, once the pore has opened, the Cl ions move very fast through the membrane so as to establish near charge equilibrium. Full charge equilibrium is never established because once the electrochemical gradient has decreased sufficiently, diffusion events become extremely rare and are not observable over the time scale of the simulation.

VII. CONCLUSION

MD simulations using NAMD were used to investigate the permeability of ions through the POPC lipid bilayer membrane. The key findings of our investigations are as follows. Na ions have an affinity to bind to atoms at or just below the POPC bilayer surface. This is in contrast with the Cl ions which do not show any tendency to bind to the bilayer surface molecules. Electrochemical potential gradients allow for the diffusion of both Na and Cl ions across the bilayer membrane. The diffusion of ions is through the opening of a water pore in the membrane.

By monitoring the ion trajectories, we have been able to show that both Na and Cl ions diffuse rapidly through the water pore that is created in the presence of high electrochemical potential gradients, with diffusion coefficients up to thirty times larger than in water. Thus, although the Na ions are the first to begin the permeation process due to the lower potential barrier it experiences, the Cl ions complete the permeation more quickly due to their faster diffusion rates. Our results confirm the findings of Gurtovenko and Vattulainen[17] who noted that ion transport is sensitive to the type of ions. Also, the faster diffusion rates of the Cl ions are in agreement with their conclusion that the strong interaction of the Na ions with the lipid head groups considerably slow down their permeation through the water pores. By determining the diffusion coefficients, we have able to quantify these effects. Finally, we have observed that while the water molecules also diffuse faster through the pore than in water, the increase in its diffusion coefficient is less than that of both the Cl and Na ions.

ACKNOWLEDGMENTS

Most of the MD simulations were carried out on the ARCCA computing facilities at Cardiff University. Rangeen

Salih acknowledges financial support from the Ministry of Higher Education and Scientific Research, Kurdistan region, Iraq and from the Cardiff University. We also acknowledge fruitful discussions with Jeffrey Comer from the Kansas State University.

[1]R. Randel, H. C. Loebl, and C. C. Matthai, "Molecular dynamics simulations of polymer translocations," Macromol. Theory Simul. **13**(5), 387–391 (2004).
[2]H. Loebl and C. Matthai, "Simulation studies of protein translocation in mitochondria," Phys. A **342**(3-4), 612–622 (2004).
[3]C. C. Matthai and N. H. March, "The application of condensed matter methods to the study of the conformation and elastic properties of biopolymers and the transport of DNA through cell membranes," Theor. Chem. Acc. **130**(4-6), 1155–1167 (2011).
[4]N. H. March and C. C. Matthai, "The application of quantum chemistry and condensed matter theory in studying amino-acids, protein folding and anticancer drug technology," Theor. Chem. Acc. **125**(3-6), 193–201 (2010).
[5]J. R. Jones, D. L. G. Rowlands, and C. B. Monk, "Diffusion coefficient of water in water and in some alkaline earth chloride solutions at 25 °C," Trans. Faraday Soc. **61**, 1384–1388 (1965).
[6]L. G. Longsworth, "The mutual diffusion of light and heavy water," J. Phys. Chem. **64**(12), 1914–1917 (1960).
[7]J. H. Wang, "Effect of ions on the self-diffusion and structure of water in aqueous electrolytic solutions," J. Phys. Chem. **58**(9), 686–692 (1954).
[8]J. H. Wang, "Self-diffusion structure of liquid water. II. Measurement of self-diffusion of liquid water with O^{18} as tracer," J. Am. Chem. Soc. **73**(9), 4181–4183 (1951).
[9]M. Holz, S. R. Heil, and A. Sacco, "Temperature-dependent self-diffusion coefficients of water and six selected molecular liquids for calibration in accurate ^{1}H NMR PFG measurements," Phys. Chem. Chem. Phys. **2**(20), 4740–4742 (2000).
[10]R. Mills, "Self-diffusion in normal and heavy water in the range 1-45.deg.," J. Phys. Chem. **77**(5), 685–688 (1973).
[11]P. Mark and L. Nilsson, "Structure and dynamics of the TIP3P, SPC, and SPC/E water models at 298 K," J. Phys. Chem. A **105**(43), 9954–9960 (2001).
[12]C. Yeh and G. Hummer, "System-size dependence of diffusion coefficients and viscosities from molecular dynamics simulations with periodic boundary conditions," J. Phys. Chem. B **108**(40), 15873–15879 (2004).
[13]J. Postma, Ph.D. thesis, University Rijkuniversiteit Groningen, The Netherlands, 1985.
[14]J. J. López Cascales, J. García de la Torre, S. J. Marrink, and H. J. C. Berendsen, "Molecular dynamics simulation of a charged biological membrane," J. Chem. Phys. **104**, 2713–2720 (1996).
[15]D. J. Hardy, Z. Wu, J. C. Phillips, J. E. Stone, R. D. Skeel, and K. Schulten, "Multilevel summation method for electrostatic force evaluation," J. Chem. Theory Comput. **11**(2), 766–779 (2015).
[16]A. A. Gurtovenko and I. Vattulainen, "Membrane potential and electrostatics of phospholipid bilayers with asymmetric transmembrane distribution of anionic lipids," J. Phys. Chem. B **112**(15), 4629–4634 (2008).
[17]A. A. Gurtovenko and I. Vattulainen, "Ion leakage through transient water pores in protein-free lipid membranes driven by transmembrane ionic charge imbalance," Biophys. J. **92**(6), 1878–1890 (2007).
[18]W. Humphrey, A. Dalke, and K. Schulten, "VMD: Visual molecular dynamics," J. Mol. Graphics **14**, 33–38 (1996).
[19]J. C. Phillips, R. Braun, W. Wang, J. Gumbart, E. Tajkhorshid, E. Villa, C. Chipot, R. D. Skeel, L. Kalel, and K. Schulten, "Scalable molecular dynamics with NAMD," J. Comput. Chem. **26**(16), 1781–1802 (2005).
[20]G. J. Martyna, D. J. Tobias, and M. L. Klein, "Constant pressure molecular dynamics algorithms," J. Chem. Phys. **101**(5), 4177–4189 (1994).
[21]P. P. Ewald, "Die Berechnung optischer und elektrostatischer Gitterpotentiale," Ann. Phys. **369**(3), 253–287 (1921).
[22]R. B. Best, X. Zhu, J. Shim, P. E. M. Lopes, J. Mittal, M. Feig, and A. D. MacKerell, "Optimization of the additive CHARMM all-atom protein force field targeting improved sampling of the backbone ϕ, ψ and side-chain χ_1 and χ_2 dihedral angles," J. Chem. Theory Comput. **8**(9), 3257–3273 (2012).
[23]N. Kučerka, S. Tristram-Nagle, and J. F. Nagle, "Structure of fully hydrated fluid phase lipid bilayers with monounsaturated chains," J. Membr. Biol. **208**(3), 193–202 (2006).
[24]J. B. Klauda, R. M. Venable, J. Alfredo Freites, J. W. O'Connor, D. J. Tobias, C. Mondragon-Ramirez, I. Vorobyov, A. D. MacKerell, and R. W. Pastor, "Update of the CHARMM all-atom additive force field for lipids: Validation on six lipid types," J. Phys. Chem. B **114**(23), 7830–7843 (2010).
[25]D. Frenkel and B. Smit, *Understanding Molecular Simulation: From Algorithms to Applications* (Academic Press, 2001).
[26]U. Essmann, L. Perera, M. L. Berkowitz, T. Darden, H. Lee, and L. G. Pedersen, "A smooth particle mesh Ewald method," J. Chem. Phys. **103**(19), 8577–8593 (1995).
[27]E. L. Cussler, *Diffusion: Mass Transfer in Fluid Systems*, Cambridge Series in Chemical Engineering (Cambridge University Press, 2009).
[28]E. Samson, J. Marchand, and K. A. Snuder, "Calculation of ionic diffusion coefficients on the basis of migration test results," Mater. Struct. **36**(257), 156–165 (2003).
[29]J. Comer, K. Schulten, and C. Chipot, "Calculation of lipid-bilayer permeabilities using an average force," J. Chem. Theory Comput. **10**(2), 554–564 (2014).
[30]R. A. Böckmann, A. Hac, T. Heimburg, and H. Grubmüller, "Effect of sodium chloride on a lipid bilayer," Biophys. J. **85**(3), 1647–1655 (2003).
[31]M. S. Miettinen, A. A. Gurtovenko, I. Vattulainen, and M. Karttunen, "Ion dynamics in cationic lipid bilayer systems in saline solutions," J. Phys. Chem. B **113**(27), 9226–9234 (2009).
[32]J. N. Sachs and T. B. Woolf, "Understanding the Hofmeister effect in interactions between chaotropic anions and lipid bilayers: Molecular dynamics simulations," J. Am. Chem. Soc. **125**(29), 8742–8743 (2003).
[33]I. V. Khavrutskii, A. A. Gorfe, B. Lu, and J. Andrew McCammon, "Free energy for the permeation of Na^+ and Cl^- ions and their ion-pair through a zwitterionic dimyristoyl phosphatidylcholine lipid bilayer by umbrella integration with harmonic fourier beads," J. Am. Chem. Soc. **131**(5), 1706–1716 (2009).